The Effect of 2D and 3D Cell Cultures on E-Cadherin Profile and Drug Resistance in Huh7 Cell

Jiaqi Shao (51184300160@stu.ecnu.edu.cn)
East China Normal University https://orcid.org/0000-0001-9268-3432
Haoyu Zou
East China Normal University
Jing Ye
East China Normal University
Meixia Zhou
East China Normal University
Lei Yu
East China Normal University https://orcid.org/0000-0002-1467-9662
Zhiqiang Yan
East China Normal University

Research Article

Keywords: E-cadherin, 3D culture, spheroids, monolayers, drug resistance, hepatocellular carcinoma

Posted Date: March 10th, 2021

DOI: https://doi.org/10.21203/rs.3.rs-260739/v1

Abstract

Studies have validated three-dimensional (3D) culture of cells differs significantly from the two-dimensional (2D) model in terms of drug efficacy due to complex mechanisms, including up-regulation of drug efflux, acquisition of stem cell-like properties by the cancer cells, aberrant apoptotic, etc. This study aimed to delineate the change of expression profile of E-cadherin in hepatoma cells Huh7 under the 3D condition and 2D condition. Cells were culture in ultra-low attachment plates to form multicellular 3D spheroids. The expression profile of E-cadherin and drug resistance were compared between 2D monolayers and 3D spheroids. E-cadherin was located at cell boundaries and cell membrane in 3D spheroids of Huh7 cells, however, E-cadherin was expressed on the cytoplasm and nuclei in 2D monolayers. In addition, high expression of E-cadherin and hepatic stem cell markers were found in 3D spheroids, and 3D spheroids showed greater resistance to pharmacological compounds. It seems 3D culture promoted the membrane localization of E-cadherin, and the change of MDR-related markers enhanced resistance in Huh7 3D spheroids. This study increases the knowledge of the effect of 3D arrangement in cancer cells.

Introduction

Hepatocellular carcinoma (HCC) is the most common primary hepatic carcinoma with a high recurrence rate and poor prognosis [1, 2]. In recent years, with the widespread occurrence of hepatitis C and non-alcoholic steatohepatitis, the incidence of HCC has continued to rise. According to statistics, the 5-year prognostic survival rate of hepatoma patients is less than 20% [3, 4]. HCC is a heterogeneous malignancy with complex carcinogenesis. Although there has been tremendous progress in the treatment of hepatocellular carcinoma over the past decades, the acquisition of chemoresistance continues to be a major hindrance in chemotherapy and targeted-based treatment of the disease [5], and resistance to these treatments can be subcategorized into intrinsic and acquired. Intrinsic resistance is pre-existent before chemotherapy, thus inducing certain treatments useless. Acquired resistance occurs gradually during the course of chemotherapy, and seems to be the main reason for tumor treatment failure [6, 7]. Monolayer/ two-dimensional (2D) culture of cancer cells is a widely used biological model for studying cancer biology and the efficacy of anti-cancer drugs. However, cells under non-physiological conditions cannot reflect the actual microenvironment in which the cells reside in the tissue [8]. There are concentration gradient changes in oxygen, pH, and soluble components (such as nutrients, effector molecules, and cell metabolites) in tumor tissues [9, 10], which affect cell proliferation, metabolism, and anti-apoptotic physiological performance. Three-dimensional (3D) culture conditions are becoming increasingly popular due to their ability to mimic tissue-like structures more effectively than the monolayer cultures, particularly in cancer and stem cell research, the natural cell characteristics and architectures are closely mimicked by the 3D cell models [8].

Multidrug resistance (MDR) is a multifactorial process that can be due to complex mechanisms, including up-regulation of drug efflux, acquisition of stem cell-like properties by the cancer cells, in

addition to reduced drug uptake, metabolic alterations, aberrant apoptotic and autophagic signaling, and changes in the tumor microenvironment [7, 11]. Studies have indicated that CSCs play a pivotal role in the emergence of MDR, which is the main cause of tumor treatment failure [9, 12-15]. In addition, CSCs in 3D culture display different types of tumor biology, including tissue invasion, metastasis drug resistance, and epithelial-mesenchymal transition (EMT) [6, 16]. ATP-binding cassette subfamily B member 1 (ABCB-1), also referred to as P-gp, is a well-studied drug efflux protein that protects organs from toxic foreign substances and toxic substances through the energy-dependent efflux of drugs from the substrate. MDR cancer cells overexpressing ABCB-1 display variations in invasive and metastatic behavior, and overexpressing ABCB-1 has been associated with poor clinical response and MDR in patients with HCC [12, 17, 18]. One of the key mechanisms of chemotherapy treatment is inducing cancer cell apoptosis, therefore, disruption of apoptotic signals is a major obstacle in the success of chemotherapy. Mutation or inactivation of pro-apoptotic factors can result in chemotherapy resistance in cancer via suppression of apoptotic pathways [19].

Epithelial cadherin (E-cadherin) is critical in cellular connectivity, it helps to form a tightly polarized cell layer to perform barrier and transport functions [20]. Calcium-dependent interactions between E-cadherin molecules connect the extracellular regions of epithelial cells to ensure that cells bind to each other in the tissue. Other E-cadherin molecules on the cell form a stable dimer structure, forming an adhesion connection in the presence of Ca^{2+} [21, 22]. E-cadherin plays a key role in maintaining homeostasis and inhibiting the occurrence of hepatoma, the losing expression of E-cadherin leads to an accelerated proliferation of hepatoma cells and is associated with increased expression of stem cell markers [23-25]. 3D culture regulates the expression of cell adhesion-related proteins in the matrix (integrin) and intercellular adhesion (E-cadherin) by simulating the microenvironment under physiological conditions [26], promoting cell differentiation and responding to the extracellular matrix (ECM) components change cell signaling pathways.

In this study, we investigated the expression profile of E-cadherin under 2D and 3D culture conditions. It was found that drug resistance of Huh7 cells was increased under 3D conditions, and the expression of genes associated with MDR was analyzed to explore the possible mechanisms of resistance in 3D spheroid. This study describes how 3D arrangement could influence the phenotype of hepatocellular carcinoma cells, increasing the knowledge of the effect of 3D arrangement in cancer cells.

Materials And Methods

Three-dimensional culture of Huh7 cells.

Huh7 cells (purchased from the Cell Resource Center, Shanghai Institutes for Biological Sciences, Chinese Academy of Sciences) were cultured in DMEM medium (Gibco) supplemented with 10% fetal bovine serum (Biological Industries), 100 u/ml penicillin, 100 u/ml streptomycin (Thermo Fisher Scientific, Cat.No.10378016). All cells were cultured at 37°C in a humidified atmosphere with 5% CO_2 and were in

the logarithmic growth phase upon initiation of the experiments. 0.25% trypsin-EDTA solution were used for digestion, and cell suspension was centrifuged at 350 × g for 5 min. For 3D culture, cells were culture in ultra-low attachment plates Corning® Spheroid Microplates (Cat. No. 4515) to form spheroids, and five thousand cells were seeded in per well. Changed the medium every other day (using the pipette tip to lightly stick to the inner wall of the hole, so as not to destroy the complete structure of spheroids).

Scanning electron microscope (SEM) analysis of 3D spheroids and monolayer cells.

The protocol of SEM sample preparations reported by Murtey et al was used in this study [27]. Briefly, (1) dehydration and drying: 3D spheroids and cells grown on coverslips (2D) were fixed with 2.5% glutaraldehyde. Continuously change the ethanol from low to high concentrations (35%, 50%, 75%, 95%, 100%) in order to replace the water in samples. For further dehydration and drying, samples were transferred to hexamethyldisilazane (HMDS) in a fume hood overnight. (2) Metal sputtering: samples were mounted onto an SEM sample stub with double-sided sticky tape. Sputter the sample with about 10 nm of gold before viewing it in the SEM. The microscopic examination was performed under the scanning electron microscope (JEOL, HITACHI-S-4800).

Immunofluorescence staining.

Spheroids and cells grown on coverslips were fixed with paraformaldehyde (4%) for 15 min and then washed with PBS. Cells grown on coverslips and spheroids were blocked in buffer (1× PBS / 5% regular serum / 0.3% Triton™ X-100) at room temperature for 60 mins. Primary antibody E-Cadherin (Cell Signaling Technology, (4A2) Mouse mAb #14472, 1:50) was incubated at 4°C overnight. The next day, fluorescent substance labeled secondary antibody (Abcam, ab150116, 1:200) was incubated for 2 h at room temperature in dark according to the manufacturer's protocol. Nuclei were counterstained with DAPI (SIGMA, 1:100). 3D spheroids were put into OCT (optimal cutting temperature compound) embedding agent for frozen section processing after immunofluorescence staining. Confocal fluorescence images were recorded on a Leica-SP8 with a 63× immersion objective.

Reverse transcription-quantitative polymerase chain reaction (RT-qPCR).

Cells were cultured for 10 days and collected to extract total RNA with an RNAprep Pure Cell Kit (TIANGEN, Beijing, China) according to the manufacturer's instructions. To determine the mRNA expression level in different culture methods, cDNA was synthesized with a PrimeScript RT reagent Kit (TAKARA, Dalian, China). Quantitative RT-PCR was performed using a SYBRB® Premix Ex Taq™ Kit (TAKARA, Dalian, China) on a CFX96™ Real-Time System (BIO-RAD, United States). The sequence of

qPCR primer was shown in Table 1. The gene expression level relative to β-actin was calculated by the 2-ΔΔCt method.

Western blot.

After the cells were collected, RIPA buffer was used to prepare cell lysis buffer, then cells were incubated on ice for 30 min to fully lyse. protein concentration was measured using the BCA assay kit from Thermo Fisher Scientific. 30 ug protein sample were loaded on sodium dodecyl sulfate polyacrylamide gels and started to electrophoresis, then transferred to PVDF membrane (ice bath during electrophoresis). The blotted PVDF membrane was incubated and blocked with 5% BSA solution at room temperature for 1 h. Incubated the E-cadherin (Cell Signaling Technology, 1:1000) with the PVDF membrane at 4°C overnight. The peroxidase-labeled secondary antibody was diluted with PBST, the PVDF membrane was incubated for 1 h at room temperature, and then washed with PBST. Added super-sensitive developer dropwise to the PVDF membrane for protein development. The relative protein expression levels were normalized to that of β-actin.

Drug sensitivity test.

Huh7 cells were seeded into 96-well spheroid microplates (Cat.No.4515) and 96-well monolayer plates at 5000 cells/well. For 3D culture, cells were cultured for 24-48 h and were observed under a phase-contrast microscope (OLYMPUS, Cat. No. IX71) to confirm that they had gathered into spheroids in each well. Sorafenib was prepared as a storage solution with DMSO (SIGMA, Cat. No. D2650-100ML) and stored at -20°C. The storage solution was diluted with medium, and the final concentration of DMSO in the working solution was 0.1%. Different concentrations of Sorafenib (650 umol/l, 280 umol/l, 140 umol/l, 70 umol/l, 35 umol/l, 17.5 umol/l, 8.75 umol/L) were added to 3D spheroids and 2D monolayers. A blank control without cells (complete medium with 0.1% DMSO), a positive control (doxorubicin, 900 umol/l), and a negative control without the drug were set to control error range. After 48 h, added CCK8 detection reagent (Yeasen Biotechnology, Shanghai) and measured cell viability according to the manufacturer's instructions. The absorbance of each well was measured at the wavelength D (450-620) nm. In this study, the concept of Z'-factor was used to ensure the detection efficiency within the same number of test repetitions, and data can be used only if $0.5 \leq Z' \text{-factor} \leq 1$. The formula for cell viability and Z'-factor were as follows:

$$\text{Cell viability } \% = \left(\frac{\text{test - blank}}{\text{negative - blank}} \right) \times 100\%$$

$$Z'\text{-factor} = \frac{(3\delta_p + 3\delta_n)}{|\mu_p - \mu_n|}$$

Where δ is the standard deviation of the average, μ is the average, p is positive, n is negative.

Statistical analysis.

All data were statistically analyzed using GraphPad Prism 7.0 software, and the statistical results were expressed as mean ± standard deviation (x ± s). In the drug sensitivity experiment, the dose curve was fitted using the 3PLFT model (when the top value ≥ 120%, fixed the top value to 100%; when the bottoms value was ≤ -20%, fix the bottom to 0%). Comparison between 2D monolayers and 3D spheroids were calculated using independent samples two-tailed *t*-test. The results of Western blot were analyzed by using Adobe Photoshop CC image analysis software to analyze the gray value. Multiple comparisons were used for comparison of given two groups after two-way ANOVA test. $P < 0.05$ was considered as significant difference.

Result

Formation of 3D structure.

The formation of spheroids with uniform size and shape was necessary for drug testing and statistical analysis. In this regard, spheroids in each well were observed through an inverted microscope. Huh7 cells spontaneously formed multicellular agglomerated spheroids when cultured for 24 h without exogenous ECM components (Fig. 1a). At this time, most of the cells were mainly concentrated in the center of the well, and only a few cells were distributed on the edge. To further evaluated the spheroid-forming ability and stability of the 3D structure, cells were continued to grow under the 3D condition. At D3, cell cluster density increased significantly with edge cells gradually gathered toward the center. After that, the density of spheroids continued to rise, and its morphology became more regular. The diameter of the spheroids was about 470 um at D7. The 3D-assembled structure of Huh7 cells was observed by scanning electron microscope, as shown in Fig. 1b', regular spheroids with smooth surface appeared more rounder than cells cultured in 2D monolayers. In 2D culture, stretched cells with a rough surface and uneven size were observed with antennae (Fig. 1b, arrow) which were not observed in the 3D condition. What's more, the cell stretched on a flat monolayer was significantly bigger than that in 3D culture. The cell morphology in these two culture conditions indicated that the 3D environment promoted dense multicellular hepatoma spheroids formation, which was not observed on the 2D monolayers.

Huh7 cells under 3D culture showedgreater drug resistance.

Several studies have indicated that hepatocellular carcinoma lines in 3D culture show increased treatment resistance compared with those in traditional 2D culture [28-33]. To assess the drug resistance of Huh7 cells in 3D culture for a specific drug when compared with its 2D counterpart, IC_{50} was used as the measurement value of the drug's effect on cell activity. After treating with sorafenib for 48 h, the overgrowth of cells under 2D and 3D culture were hindered. It could be observed under a phase-contrast microscope (Fig. 2a), the density of the corresponding spheroids showed a downward trend as the drug concentration rose, and showing a loose sphere structure at 650 umol/L. As is shown in Fig. 2b, the IC_{50}

value of sorafenib in 3D spheroids (IC_{50} value = 23.85 umol) was much higher than that in 2D monolayers (IC_{50} value = 7.423 umol, $P < 0.001$). The results showed that the Huh7 cell line which developed 3D multicellular spheroids tended to show greater resistance to sorafenib as compared to 2D.

The expression of E-cadherin was different between 3D spheroids and 2D monolayers.

In this study, the localization of E-cadherin expression in 2D monolayers and 3D spheroids of Huh7 cells were analyzed by immunofluorescence. With the help of a laser confocal microscope, it was observed that E-cadherin in the 3D spheroids was concentrated on the boundary between the cell membrane and intercellular contact (Fig. 3a), forming a tight connection between the cells. In contrast, E-cadherin was expressed on the cytoplasm and nuclei in 2D monolayers without obvious expression on the cell boundaries. It seems the ectopic expression of E-cadherin was affected by the 3D arrangement. The expression of E-cadherin at mRNA and protein levels under two culture conditions were further examined. The mRNA of E-cadherin in 3D spheroids was increased compared with it in 2D cultures (Fig. 3b). Besides, the western blot results showed the amount of E-cadherin protein in 3D spheroids was much higher than that in 2D monolayers (Fig. 3c, $P < 0.05$), which was consistent with the gene expression results. These indicated that the expression of E-cadherin in 3D spheroids increased at both the mRNA and protein levels.

Expression of mesenchymal markers and MDR-related genes in 3D culture.

To further identify the specific phenotypic changes in 3D spheroids and 2D monolayers, mesenchymal markers was analyzed. Huh7 cells grown in 3D spheroids were detected at a lower extent of N-cadherin and α-smooth muscle actin (α-SMA) compared to 2D monolayers (Fig. 4a, $^{****}P < 0.0001$, $^{***}P < 0.001$) however, vimentin showed an opposite gene expression pattern, since it was higher in 3D spheroids ($^{**}P < 0.01$). Huh7 cells with 3D spheroids structure produced more matrix metalloproteinase-1 (MMP-1), matrix metalloproteinase-3 (MMP-3), and matrix metalloproteinase-7 (MMP-7), as determined by qPCR (Fig. 4b). ABCB-1 can reduce intracellular compound concentrations by releasing anticancer drugs to develop drug resistance including Sorafenib. As shown in Fig. 4c, the expression of drug transport gene *ABCB-1* was higher in 3D spheroids ($^{***}P < 0.001$). CSC-related markers EpCAM, CD13, CD133, CD24, CD44 were all significantly increased in 3D spheroids at mRNA level (Fig. 4d), indicating that the 3D microenvironment could induce an up-regulation of stemness genes for Huh7 cells. Cancer cells are resistant to chemotherapeutic agents via upregulating anti-apoptotic signals and downregulating pro-apoptotic signals, etc [34]. Pro-apoptotic factors PARP-1, p53, and caspases were also detected and most of them were reduced in 3D culture (Fig. 4e). The change of MDR-related genes under 3D culture might be concerned with the increased drug resistance of this model.

Discussion

The 3D culture of Huh7 cells established in this study had the characteristics of controllable size and compact spheroid structure, which provided good support for a subsequent drug sensitivity test. It was found a completely different location of E-cadherin between 2D monolayers and 3D spheroids, and E-cadherin expression was higher in 3D spheroids. Huh7 cells cultured in 3D conditions showed stronger drug resistance when forming dense 3D spheroids structure, and changes in MDR-related gene expression patterns help explain the increased resistance in 3D culture. These results provide support for the objective response to drug resistance induced by tumor cells in 3D culture.

The formation and stability of the 3D structure mainly depend on the cell-cell dynamic adhesion structure [35], and the adhesion can be reshaped according to the cell contact conditions: when the contact between cells is lacking, E-cadherin endocytosis enters the circulation; when the contact between cells is restored, the endocytosis of E-cadherin is down-regulated, and the E-cadherin molecule exits the circulation pathway [36]. Higher E-cadherin expression in 3D spheroids compared to 2D monolayers has been demonstrated in recent papers focused on prostate cancer and pancreatic adenocarcinoma cancer cells [37, 38], however, in this study, it was found that not only does the expression of E-cadherin increased in 3D spheroids of Huh7, but the location of E-cadherin also changed in 3D spheroids (Fig. 3a). Studies have shown that E-cadherin accumulates in the nuclei may regulate gene transcription directly [39]. The cytoplasmic tail of E-cadherin is connected to the actin cytoskeleton through β-catenin and many other molecules. β-catenin also acts as an important intermediate molecule in the Wnt signaling pathway in the cytoplasm. The occurrence of E-cadherin nuclei localization can effectively inhibit the phenotype of cancer stem cells induced by Wnt/β-catenin [40]. This is consistent with the results in this study that the expression of the stem cell markers in the 2D cultures with E-cadherin nuclei located was significantly lower than that of the 3D spheroids. Drugs diffuse to cells in the 2D monolayer equally, but drug diffusion to cells in a spheroid may be at variable concentrations depending on the depth to the surface where the cells were located [41]. Huh7 cells formed tight cell-cell adhesion junctions in 3D culture, which maintained the multi-layered structure of the 3D culture and formed a natural biological barrier. The study of Liang et al. showed that in a 3D model, E-cadherin up-regulates the expression of multidrug resistance protein through HIF-1α, leading to multicellular resistance [42]. All these studies reflect that the occurrence of drug resistance is related to the expression profile of E-cadherin.

The 3D spheroids model was validated by high drug resistance and enhanced cell migration [43]. Studies have shown cells from different tumors formed spheroids that differed in regard to EMT-related gene expression [44], but no consistent expression of EMT-related genes was found under the same culture conditions in this study. The mechanisms of EMT-induced drug resistance are not fully understood although most recent studies suggest that EMT and CSC share some similarities and their involvements in drug resistance represent different manifestations of the same phenotype [45]. In this study, CSC-related genes were increased in Huh7 3D spheroids comparing with 2D culture, which is consistent with the conclusion of existing studies that hepatoma spheroids with stem cell phenotype were more resistant to

chemotherapy than 2D monolayers [28]. Changes in MDR-related gene expression due to 3D arrangement, such as MMPs upregulated in Huh7 3D spheroids may indicate that the 3D spheroids with a stronger migration potential and most pro-apoptotic factors determined at a lower extent in 3D culture indicated that the apoptosis level of cells decreased under 3D culture.

Studies have validated 3D culture of cells differs significantly from the 2D model in terms of drug efficacy [46-49]. 3D culture simulates the microenvironment of tissue center necrosis and extracellular matrix microenvironment of tumor tissue induced by chemotherapy drugs, and better reflect the heterogeneity of tumor cells and drug sensitivity. Besides, differences in the distribution of reactive oxygen species, expression of MDR genes, cell-cell and cell-matrix adhesion may all be attributable to differences in drug resistance between 3D culture and 2D culture [50, 51]. 3D hepatoma spheroids are expected to be used as a drug detection platform for HCC in vitro [52], but the mechanism by which the 3D culture affects the increase of drug resistance of hepatoma cells needs further research. In recent years, the development of 3D culture technology has grown exponentially, providing a broad application prospect in drug development and prediction of chemotherapy response in cancer patients. This study provides theoretical support for 3D culture to objectively respond to drug resistance generated by chemotherapy drugs induced by the tumor. In the future, the 3D hepatoma model may be a better platform for in vitro drug detection, making us closer to the goal of personalized medicine.

Abbreviations

E-cadherin: epithelial cadherin; 3D: three-dimensional; 2D: two-dimensional; HCC: hepatocellular carcinoma; IC_{50}: half maximal inhibitory concentration; EpCAM: epithelial cell adhesion molecule; α-SMA: α-smooth muscle actin; MDR: multidrug resistance; CSCs: cancer stem cells; ECM: extracellular matrix; ABCB-1: ATP-binding cassette subfamily B member 1; DAPI: 4',6-diamidino-2-phenylindole; DMEM: Dulbecco's modified eagle's media; PBS: phosphate buffered saline; DMSO: dimethyl sulfoxide; HMDS: hexamethyldisilazane; MMP: matrix metalloproteinase; PARP-1: poly (ADP-ribose) polymerase 1;

Declarations

Funding

This work was supported by the National Natural Science Foundation of China under Grant 81872812 and 82073800; "985" grants of East China Normal University (ECNU).

Competing interests

No competing financial interests exist

Availability of data and materials

All data generated or analysed during this study are included in this published article or are available from the corresponding author on reasonable request.

Code availability

Not applicable

Authors' contributions

All authors contributed to the study conception and design. Material preparation, data collection and analysis were performed by Jiaqi Shao. The first draft of the manuscript was written by Jiaqi Shao, and Haoyu Zou. All authors commented on previous versions of the manuscript. All authors read and approved the final manuscript.

Ethics approval

Not applicable

Patient consent for publication

Not applicable

Consent to participate

Not applicable

Consent for publication

Not applicable

Refenence

1. Balogh J, Victor D, 3rd, Asham EH, Burroughs SG, Boktour M, Saharia A, Li X, Ghobrial RM and Monsour HP, Jr. (2016) Hepatocellular carcinoma: a review. J Hepatocell Carcinoma 3:41-53. doi: 10.2147/JHC.S61146
2. Zhu RX, Seto WK, Lai CL and Yuen MF (2016) Epidemiology of Hepatocellular Carcinoma in the Asia-Pacific Region. Gut Liver 10:332-9. doi: 10.5009/gnl15257
3. Toosi AE (2015) Liver Fibrosis: Causes and Methods of Assessment, A Review. Rom J Intern Med 53:304-14. doi: 10.1515/rjim-2015-0039
4. Siegel RL, Miller KD and Jemal A (2020) Cancer statistics, 2020. CA Cancer J Clin 70:7-30. doi: 10.3322/caac.21590
5. Marin JJG, Macias RIR, Monte MJ, Romero MR, Asensio M, Sanchez-Martin A, Cives-Losada C, Temprano AG, Espinosa-Escudero R, Reviejo M, Bohorquez LH and Briz O (2020) Molecular Bases of

Drug Resistance in Hepatocellular Carcinoma. Cancers (Basel) 12. doi: 10.3390/cancers12061663

6. Zhang C, Yang Z, Dong D-L, Jang T-S, Knowles JC, Kim H-W, Jin G-Z and Xuan Y (2020) 3D culture technologies of cancer stem cells: promising ex vivo tumor models. Journal of tissue engineering 11:2041731420933407-2041731420933407. doi: 10.1177/2041731420933407
7. Garcia-Mayea Y, Mir C, Masson F, Paciucci R and ME LL (2020) Insights into new mechanisms and models of cancer stem cell multidrug resistance. Semin Cancer Biol 60:166-180. doi: 10.1016/j.semcancer.2019.07.022
8. Chaicharoenaudomrung N, Kunhorm P and Noisa P (2019) Three-dimensional cell culture systems as an in vitro platform for cancer and stem cell modeling. World J Stem Cells 11:1065-1083. doi: 10.4252/wjsc.v11.i12.1065
9. Langhans SA (2018) Three-Dimensional in Vitro Cell Culture Models in Drug Discovery and Drug Repositioning. Front Pharmacol 9:6. doi: 10.3389/fphar.2018.00006
10. Amaral RLF, Miranda M, Marcato PD and Swiech K (2017) Comparative Analysis of 3D Bladder Tumor Spheroids Obtained by Forced Floating and Hanging Drop Methods for Drug Screening. Front Physiol 8:605. doi: 10.3389/fphys.2017.00605
11. Bukowski K, Kciuk M and Kontek R (2020) Mechanisms of Multidrug Resistance in Cancer Chemotherapy. International journal of molecular sciences 21:3233. doi: 10.3390/ijms21093233
12. Li J, Duan B, Guo Y, Zhou R, Sun J, Bie B, Yang S, Huang C, Yang J and Li Z (2018) Baicalein sensitizes hepatocellular carcinoma cells to 5-FU and Epirubicin by activating apoptosis and ameliorating P-glycoprotein activity. Biomed Pharmacother 98:806-812. doi: 10.1016/j.biopha.2018.01.002
13. Chen Y, Yu D, Zhang H, He H, Zhang C, Zhao W and Shao RG (2012) CD133(+)EpCAM(+) phenotype possesses more characteristics of tumor initiating cells in hepatocellular carcinoma Huh7 cells. Int J Biol Sci 8:992-1004. doi: 10.7150/ijbs.4454
14. Ma S, Lee TK, Zheng BJ, Chan KW and Guan XY (2008) CD133+ HCC cancer stem cells confer chemoresistance by preferential expression of the Akt/PKB survival pathway. Oncogene 27:1749-58. doi: 10.1038/sj.onc.1210811
15. Yamashita T, Ji J, Budhu A, Forgues M, Yang W, Wang HY, Jia H, Ye Q, Qin LX, Wauthier E, Reid LM, Minato H, Honda M, Kaneko S, Tang ZY and Wang XW (2009) EpCAM-positive hepatocellular carcinoma cells are tumor-initiating cells with stem/progenitor cell features. Gastroenterology 136:1012-24. doi: 10.1053/j.gastro.2008.12.004
16. Zhao Y, Dong Q, Li J, Zhang K, Qin J, Zhao J, Sun Q, Wang Z, Wartmann T, Jauch KW, Nelson PJ, Qin L and Bruns C (2018) Targeting cancer stem cells and their niche: perspectives for future therapeutic targets and strategies. Semin Cancer Biol 53:139-155. doi: 10.1016/j.semcancer.2018.08.002
17. Ceballos MP, Rigalli JP, Cere LI, Semeniuk M, Catania VA and Ruiz ML (2019) ABC Transporters: Regulation and Association with Multidrug Resistance in Hepatocellular Carcinoma and Colorectal Carcinoma. Curr Med Chem 26:1224-1250. doi: 10.2174/0929867325666180105103637

18. Kong J, Qiu Y, Li Y, Zhang H and Wang W (2019) TGF-beta1 elevates P-gp and BCRP in hepatocellular carcinoma through HOTAIR/miR-145 axis. Biopharm Drug Dispos 40:70-80. doi: 10.1002/bdd.2172
19. Li S, Gao M, Li Z, Song L, Gao X, Han J, Wang F, Chen Y, Li W and Yang J (2018) p53 and P-glycoprotein influence chemoresistance in hepatocellular carcinoma. Front Biosci (Elite Ed) 10:461-468.
20. Gumbiner BM (2005) Regulation of cadherin-mediated adhesion in morphogenesis. Nat Rev Mol Cell Biol 6:622-34. doi: 10.1038/nrm1699
21. Pertz O, Bozic D, Koch AW, Fauser C, Brancaccio A and Engel J (1999) A new crystal structure, Ca2+ dependence and mutational analysis reveal molecular details of E-cadherin homoassociation. EMBO J 18:1738-47. doi: 10.1093/emboj/18.7.1738
22. Wu Y, Jin X, Harrison O, Shapiro L, Honig BH and Ben-Shaul A (2010) Cooperativity between trans and cis interactions in cadherin-mediated junction formation. Proc Natl Acad Sci U S A 107:17592-7. doi: 10.1073/pnas.1011247107
23. Maeda S and Nakagawa H (2015) Roles of E-cadherin in Hepatocarcinogenesis. In: Nakao K, Minato N and Uemoto S (eds) Innovative Medicine: Basic Research and Development, Tokyo pp. 71-77
24. Nakagawa H, Hikiba Y, Hirata Y, Font-Burgada J, Sakamoto K, Hayakawa Y, Taniguchi K, Umemura A, Kinoshita H, Sakitani K, Nishikawa Y, Hirano K, Ikenoue T, Ijichi H, Dhar D, Shibata W, Akanuma M, Koike K, Karin M and Maeda S (2014) Loss of liver E-cadherin induces sclerosing cholangitis and promotes carcinogenesis. Proc Natl Acad Sci U S A 111:1090-5. doi: 10.1073/pnas.1322731111
25. Schneider MR, Hiltwein F, Grill J, Blum H, Krebs S, Klanner A, Bauersachs S, Bruns C, Longerich T, Horst D, Brandl L, de Toni E, Herbst A and Kolligs FT (2014) Evidence for a role of E-cadherin in suppressing liver carcinogenesis in mice and men. Carcinogenesis 35:1855-62. doi: 10.1093/carcin/bgu109
26. Santini MT, Rainaldi G and Indovina PL (2000) Apoptosis, cell adhesion and the extracellular matrix in the three-dimensional growth of multicellular tumor spheroids. Crit Rev Oncol Hematol 36:75-87. doi: 10.1016/s1040-8428(00)00078-0
27. Murtey MD and Ramasamy P (2016) Sample Preparations for Scanning Electron Microscopy – Life Sciences. Modern Electron Microscopy in Physical and Life Sciences,
28. Takai A, Fako V, Dang H, Forgues M, Yu Z, Budhu A and Wang XW (2016) Three-dimensional Organotypic Culture Models of Human Hepatocellular Carcinoma. Sci Rep 6:21174. doi: 10.1038/srep21174
29. Wu G, Zhan S, Rui C, Sho E, Shi X and Ding Y (2019) Microporous cellulosic scaffold as a spheroid culture system modulates chemotherapeutic responses and stemness in hepatocellular carcinoma. J Cell Biochem 120:5244-5255. doi: 10.1002/jcb.27799
30. Liao W, Wang J, Xu J, You F, Pan M, Xu X, Weng J, Han X, Li S, Li Y, Liang K, Peng Q and Gao Y (2019) High-throughput three-dimensional spheroid tumor model using a novel stamp-like tool. J Tissue Eng 10:2041731419889184. doi: 10.1177/2041731419889184

31. Uchida Y, Tanaka S, Aihara A, Adikrisna R, Yoshitake K, Matsumura S, Mitsunori Y, Murakata A, Noguchi N, Irie T, Kudo A, Nakamura N, Lai PB and Arii S (2010) Analogy between sphere forming ability and stemness of human hepatoma cells. Oncol Rep 24:1147-51. doi: 10.3892/or_00000966
32. Yip D and Cho CH (2013) A multicellular 3D heterospheroid model of liver tumor and stromal cells in collagen gel for anti-cancer drug testing. Biochem Biophys Res Commun 433:327-32. doi: 10.1016/j.bbrc.2013.03.008
33. Jung H-R, Kang HM, Ryu J-W, Kim D-S, Noh KH, Kim E-S, Lee H-J, Chung K-S, Cho H-S, Kim N-S, Im D-S, Lim JH and Jung C-R (2017) Cell Spheroids with Enhanced Aggressiveness to Mimic Human Liver Cancer In Vitro and In Vivo. Scientific Reports 7:10499. doi: 10.1038/s41598-017-10828-7
34. Chen L, Zeng Y and Zhou S-F (2018) Role of Apoptosis in Cancer Resistance to Chemotherapy. Current Understanding of Apoptosis - Programmed Cell Death,
35. Le TL, Yap AS and Stow JL (1999) Recycling of E-cadherin: a potential mechanism for regulating cadherin dynamics. J Cell Biol 146:219-32.
36. Haga T, Uchide N, Tugizov S and Palefsky JM (2008) Role of E-cadherin in the induction of apoptosis of HPV16-positive CaSki cervical cancer cells during multicellular tumor spheroid formation. Apoptosis 13:97-108. doi: 10.1007/s10495-007-0132-2
37. Eder T, Weber A, Neuwirt H, Grünbacher G, Ploner C, Klocker H, Sampson N and Eder IE (2016) Cancer-Associated Fibroblasts Modify the Response of Prostate Cancer Cells to Androgen and Anti-Androgens in Three-Dimensional Spheroid Culture. Int J Mol Sci 17. doi: 10.3390/ijms17091458
38. Fontana F, Raimondi M, Marzagalli M, Sommariva M, Limonta P and Gagliano N (2019) Epithelial-To-Mesenchymal Transition Markers and CD44 Isoforms Are Differently Expressed in 2D and 3D Cell Cultures of Prostate Cancer Cells. Cells 8. doi: 10.3390/cells8020143
39. Du W, Liu X, Fan G, Zhao X, Sun Y, Wang T, Zhao R, Wang G, Zhao C, Zhu Y, Ye F, Jin X, Zhang F, Zhong Z and Li X (2014) From cell membrane to the nucleus: an emerging role of E-cadherin in gene transcriptional regulation. J Cell Mol Med 18:1712-9. doi: 10.1111/jcmm.12340
40. Su YJ, Chang YW, Lin WH, Liang CL and Lee JL (2015) An aberrant nuclear localization of E-cadherin is a potent inhibitor of Wnt/beta-catenin-elicited promotion of the cancer stem cell phenotype. Oncogenesis 4:e157. doi: 10.1038/oncsis.2015.17
41. Edmondson R, Broglie JJ, Adcock AF and Yang L (2014) Three-dimensional cell culture systems and their applications in drug discovery and cell-based biosensors. Assay Drug Dev Technol 12:207-18. doi: 10.1089/adt.2014.573
42. Liang X, Xu X, Wang F, Li N and He J (2016) E-cadherin increasing multidrug resistance protein 1 via hypoxia-inducible factor-1alpha contributes to multicellular resistance in colorectal cancer. Tumour Biol 37:425-35. doi: 10.1007/s13277-015-3811-6
43. Kimlin LC, Casagrande G and Virador VM (2013) In vitro three-dimensional (3D) models in cancer research: an update. Mol Carcinog 52:167-82. doi: 10.1002/mc.21844
44. Melissaridou S, Wiechec E, Magan M, Jain MV, Chung MK, Farnebo L and Roberg K (2019) The effect of 2D and 3D cell cultures on treatment response, EMT profile and stem cell features in head and

neck cancer. Cancer Cell International 19:16. doi: 10.1186/s12935-019-0733-1

45. Shibue T and Weinberg RA (2017) EMT, CSCs, and drug resistance: the mechanistic link and clinical implications. Nat Rev Clin Oncol 14:611-629. doi: 10.1038/nrclinonc.2017.44
46. Riedl A, Schlederer M, Pudelko K, Stadler M, Walter S, Unterleuthner D, Unger C, Kramer N, Hengstschläger M, Kenner L, Pfeiffer D, Krupitza G and Dolznig H (2017) Comparison of cancer cells in 2D vs 3D culture reveals differences in AKT-mTOR-S6K signaling and drug responses. J Cell Sci 130:203-218. doi: 10.1242/jcs.188102
47. Imamura Y, Mukohara T, Shimono Y, Funakoshi Y, Chayahara N, Toyoda M, Kiyota N, Takao S, Kono S, Nakatsura T and Minami H (2015) Comparison of 2D- and 3D-culture models as drug-testing platforms in breast cancer. Oncol Rep 33:1837-43. doi: 10.3892/or.2015.3767
48. Souza AG, Silva IBB, Campos-Fernandez E, Barcelos LS, Souza JB, Marangoni K, Goulart LR and Alonso-Goulart V (2018) Comparative Assay of 2D and 3D Cell Culture Models: Proliferation, Gene Expression and Anticancer Drug Response. Curr Pharm Des 24:1689-1694. doi: 10.2174/1381612824666180404152304
49. Hou S, Tiriac H, Sridharan BP, Scampavia L, Madoux F, Seldin J, Souza GR, Watson D, Tuveson D and Spicer TP (2018) Advanced Development of Primary Pancreatic Organoid Tumor Models for High-Throughput Phenotypic Drug Screening. SLAS Discov 23:574-584. doi: 10.1177/2472555218766842
50. Vinci M, Gowan S, Boxall F, Patterson L, Zimmermann M, Court W, Lomas C, Mendiola M, Hardisson D and Eccles SA (2012) Advances in establishment and analysis of three-dimensional tumor spheroid-based functional assays for target validation and drug evaluation. BMC Biol 10:29. doi: 10.1186/1741-7007-10-29
51. Nath S and Devi GR (2016) Three-dimensional culture systems in cancer research: Focus on tumor spheroid model. Pharmacol Ther 163:94-108. doi: 10.1016/j.pharmthera.2016.03.013
52. Eilenberger C, Rothbauer M, Ehmoser E-K, Ertl P and Küpcü S (2019) Effect of Spheroidal Age on Sorafenib Diffusivity and Toxicity in a 3D HepG2 Spheroid Model. Scientific Reports 9:4863. doi: 10.1038/s41598-019-41273-3

Tables

Table 1

Primer sequence (5'-3')

Genes	Primer sequence
E-cadherin	F: ACATACACTCTCTTCTCTC R: GTCATTCTGATCGGTTAC
EpCAM	F: ATTGTGGTTGTGGTGATAG R: TCTCAGCCTTCTCATACTT
CD13	F: CACCTCTACCATCATCAG R: CCACCACCATAATCGTTA
CD24	F: AACAACAACTGGAACTTCAA R: CTTGGTGGTGGCATTAGT
CD44	F: CTGACATCAAGCAATAGG R: GTGGGTAATGAGAGGTATA
CD133	F: CAACGAGTCCTTCCTATA R: CTCTCCAACAATCCATTC
ABCB-1	F: CAATGATGCTGCTCAAGTT R: GCCAACCATAGATGAAGGA
Vimentin	F: TTGACCTTGAACGCAAAG R: GCTCCTGGATTTCCTCTT
N-cadherin	F: TCATCATCCTGCTTATCC R: ATTATCTCTTACATCATCTTCTG
α-SMA	F: GTCCAGATTCTCTTGATGATG R: AATGTGAGCACCTTCCTT
MMP1	F: GAGCTCAACTTCCGGGTAGA R: CCCAAAAGCGTGTGACAGTA
MMP3	F: CAAGGCATAGAGACAACATAGA R: GCACAGCAACAGTAGGAT
MMP7	F: GCTCAGGACTATCTCAAG R: ACATTCCAGTTATAGGTAGG
MMP14	F: AAGTGATGGATGGATACC R: AATGCTTGTCTCCTTTGA
caspase-3	F: TCGTTGTAGAAGTCTAACTG R: CCACTGTCTGTCTCAATG
caspase-7	F: GATTTGACAGCCCACTTT R: GCAAGCCTGAATGAAGAA
caspase-8	F: GAAGCAGCAGCCTTGAAG R: GAGTCCGAGATTGTCATTACC

Genes	Primer sequence
caspase-9	F: ACATTGGTTCTGGAGGAT R: AGGATGTAAGCCAAATCTG
p53	F: TCAGACCTATGGAAACTAC R: GGACAGCATCAAATCATC
PARP-1	F: ATGAAGTGGCGAAGAAGAA R: CGTCCTTGATGTTCCAGAT
β-actin	F: CATGTACGTTGCTATCCAGGC R: CTCCTTAATGTCACGCACGAT

Figures

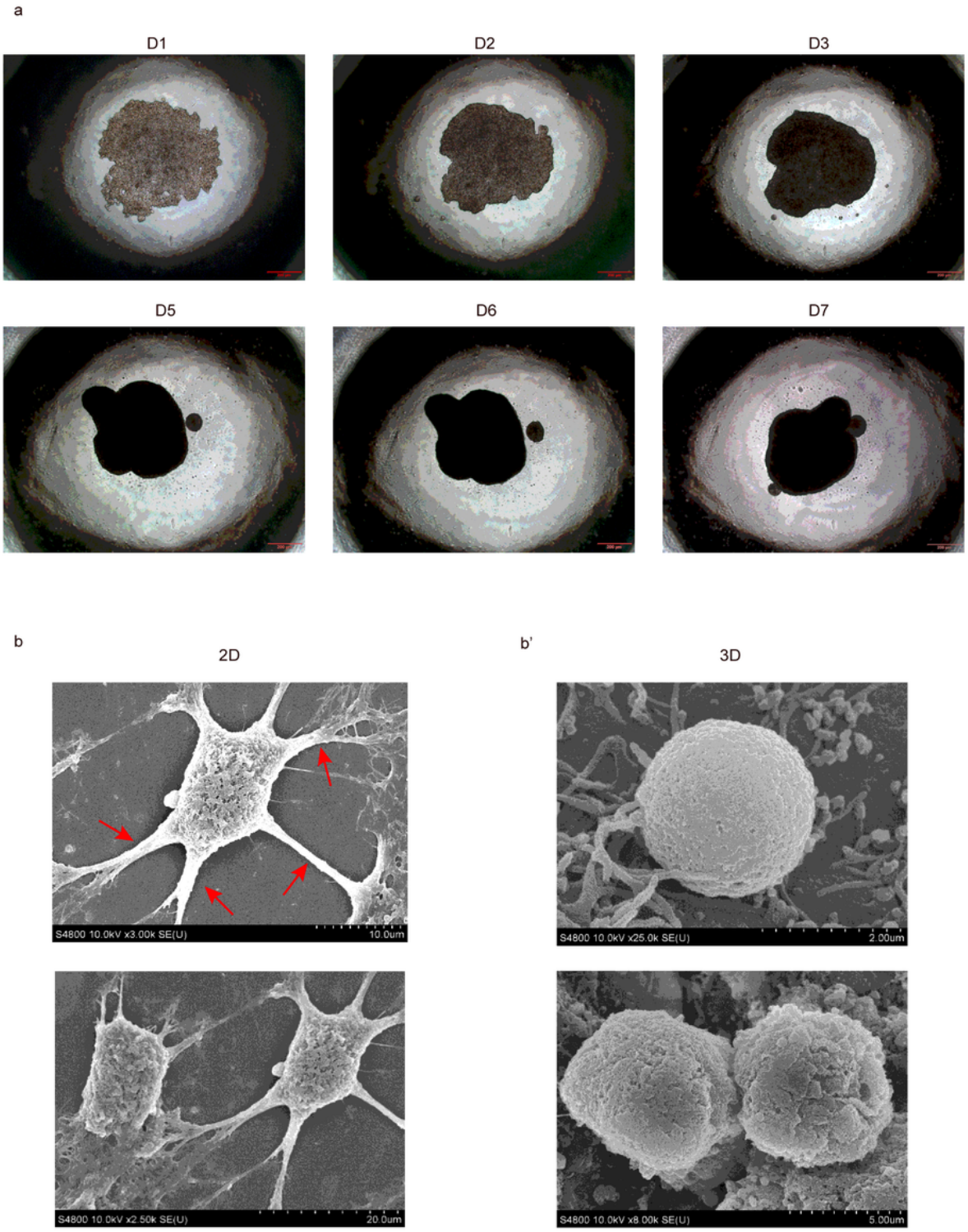

Figure 1

Morphology of 3D spheroids and 2D monolayers. (a) 3D spheroids in single well were observed by phase-contrast microscope on different days (× 40 magnification). Bar: 200 um. (b) Single cell of 3D spheroids (cells were cultured on day 7) and 2D monolayers was observed by scanning electron microscope. Bar of 2D monolayers: 10 um (top); 20 um (bottom); bar of 3D spheroids: 2 um (top); 5 um (bottom), the arrows represent antennae.

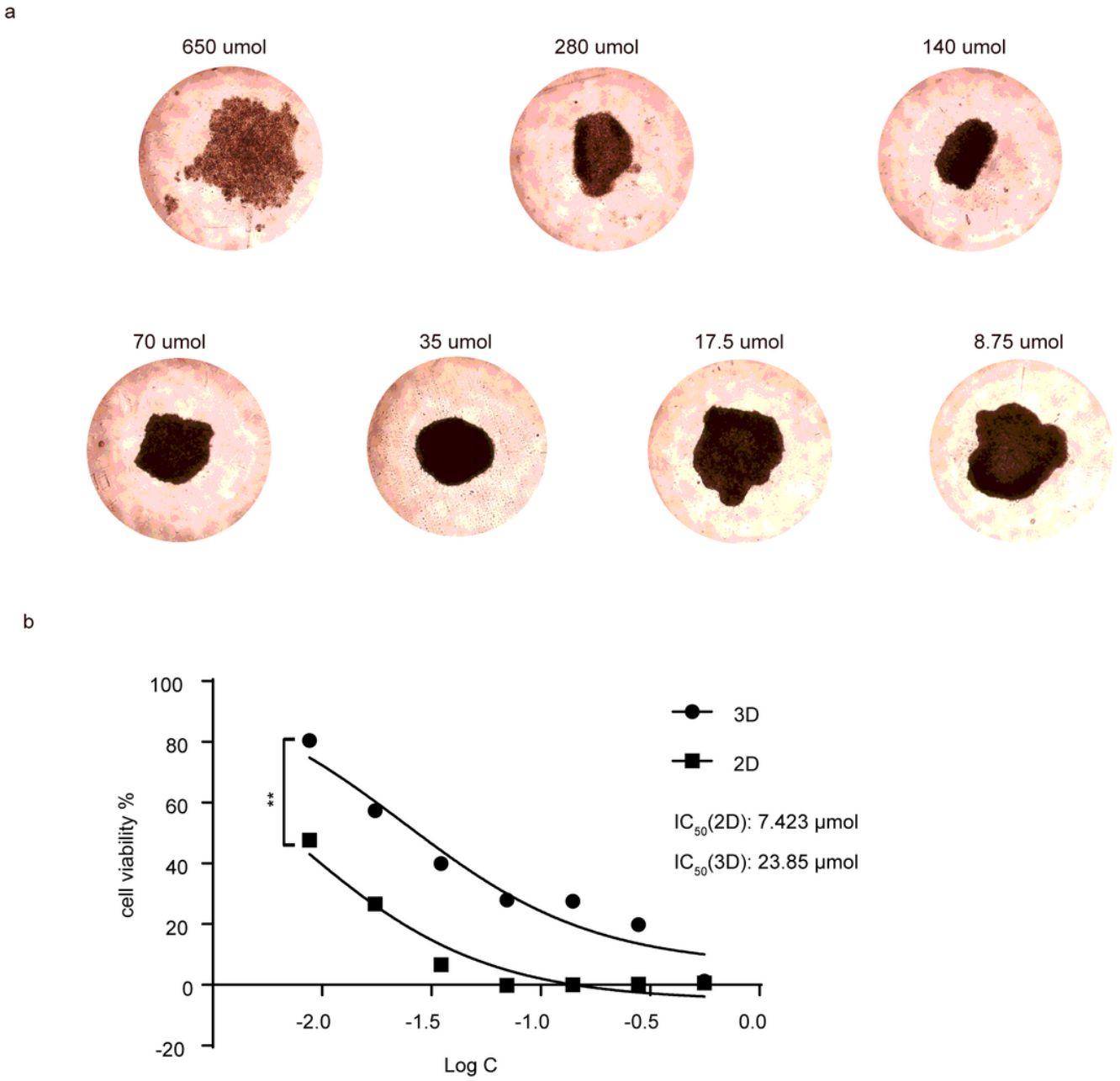

Figure 2

Drug resistance of 3D spheroids. (a) Morphology of 3D spheroids were observed by phase-contrast microscope in different drug concentrations. The drug concentrations were as follows: 650 umol, 280 umol, 140 umol, 70 umol, 35 umol, 7.5 umol, 8.75umol. Bar: 200 um. (b) The IC50 values of Sorafenib in 2D monolayers (IC50 = 7.423 umol) and 3D spheroids (IC50 = 23.85 umol). Data are means ± SD of duplicate samples, ** P < 0.01.

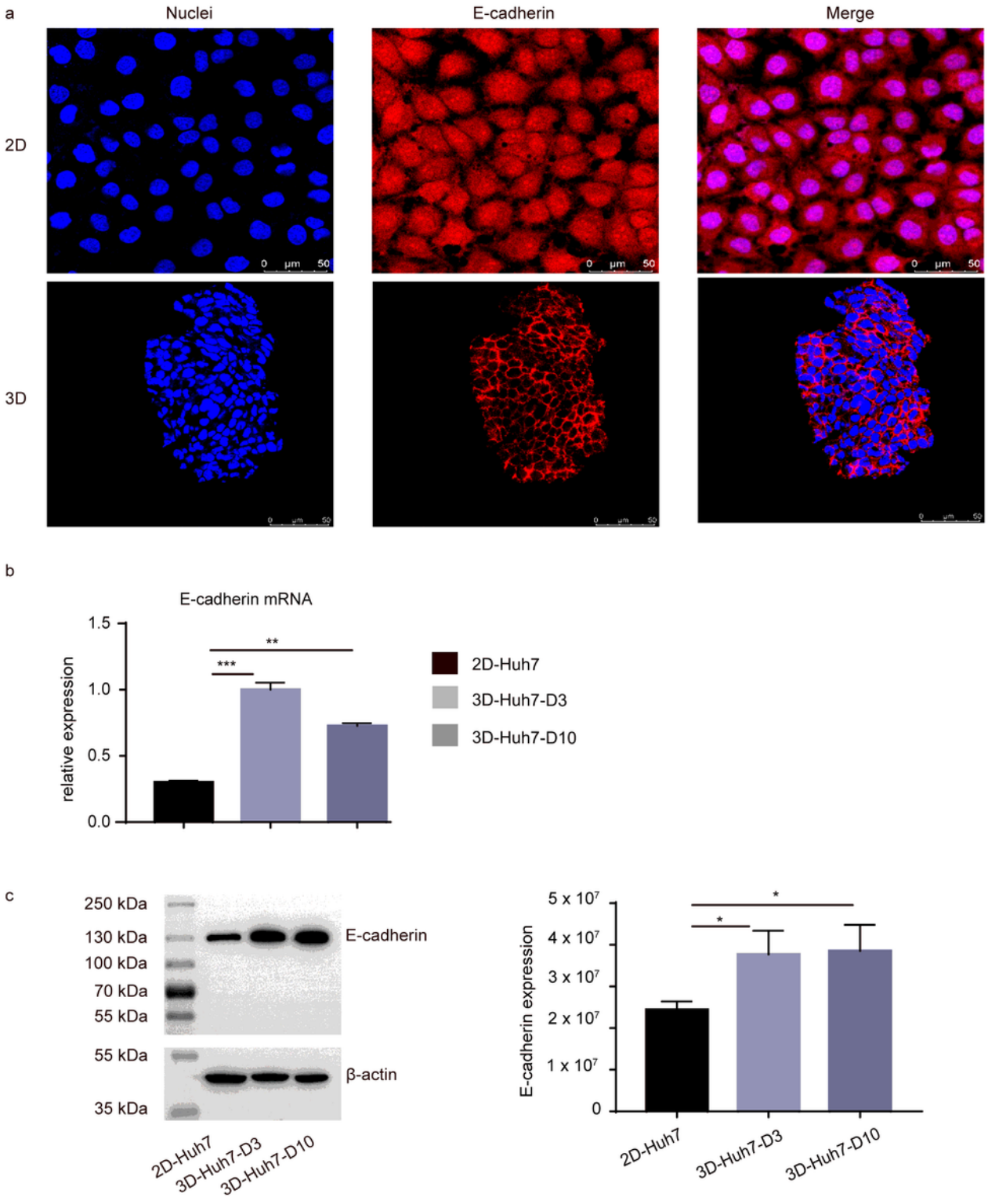

Figure 3

Expression of E-cadherin protein in 3D spheroids and 2D monolayers. (a) Immunofluorescence analysis of E-cadherin (red) localization in 3D spheroids (top) and 2D monolayers (bottom), nuclei (blue). Bar: 50 um. E-cadherin mRNA (b) and protein levels (c) in 2D and 3D models, statistical analysis of the western blot results (right). Data are means ± SD of duplicate samples, *P < 0.05, **P < 0.01, ***P < 0.001.

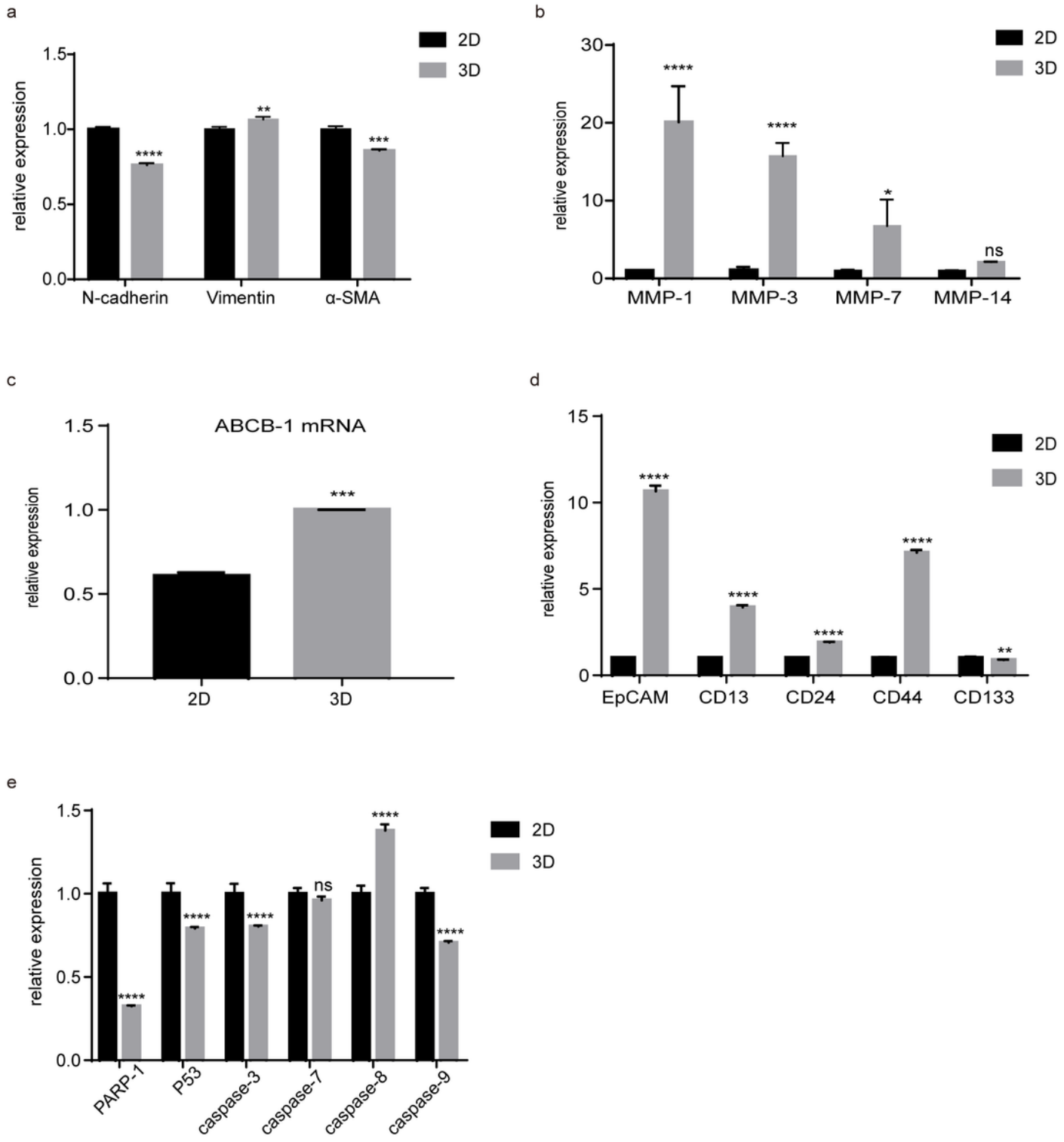

Figure 4

Expression of mesenchymal markers and MDR-related genes between 3D spheroids and 2D monolayers, detected by qPCR. (a) Expression of N-cadherin, α-SMA and Vimentin. (b) Expression of matrix metalloproteinase, MMP-1, MMP-3, MMP-7, MMP-14. (c) Expression of ABCB-1 gene. (d) Expression of stem cell markers, EpCAM, CD13, CD133, CD24, CD44. (e) Expression of apoptosis-related genes, PARP-1,

p53, caspase-3, caspase-7, caspase-8, caspase-9. Data are means ± SD of duplicate samples, *P < 0.05, **P < 0.01, ***P < 0.001, ****P < 0.0001.